Biophysical Chemistry 28 (1987) 21–34
Elsevier

BPC 01179

Variation of efficiency with free-energy dissipation in models of biological energy transduction

Davor Juretić [a,*] and Hans V. Westerhoff [b]

[a] *Biochemistry, Uniformed Services University of the Health Sciences, Bethesda, MD 20814 and* [b] *Laboratory of Molecular Biology, National Institute of Diabetes, and Digestive and Kidney Diseases, National Institutes of Health, Building 2, Room 319, Bethesda, MD 20892, U.S.A.*

Received 10 February 1987
Revised manuscript received 11 May 1987
Accepted 5 June 1987

Mosaic nonequilibrium thermodynamics; Bacteriorhodopsin; Optimization; Entropy production; Proton pumping; Slip; Coupling

For two models of biological free-energy transducers, it is investigated how free-energy dissipation and efficiency vary as (i) the demand for output free energy, (ii) the input free energy or (iii) the properties of the transducers themselves, are varied. One model is representative of near-equilibrium free-energy transducers in general, the other is a special case of far-from-equilibrium free-energy transduction, reminiscent of proton pumping by bacteriorhodopsin. It turns out that the relationship between efficiency and free-energy dissipation depends strongly on what varies. In some cases, free-energy dissipation increases as the efficiency increases. It is suggested that this is one reason why biological evolution has not resulted in high efficiencies and low rates of free-energy dissipation. For the near-equilibrium free-energy transducer, the free-energy dissipation at the static head steady state is minimal with respect to variations in the output force. For the far-from-equilibrium model (of bacteriorhodopsin), the static head does not correspond to such a minimum, if that free-energy transducer slips.

1. Introduction

Biological free-energy transducing systems dissipate free energy at a significant rate. In some cases this free-energy dissipation may be high enough to make the availability of free energy in the environment a limiting factor for the functioning of the organism [1,2]. Examples include microbial growth under catabolic limitation [2,3], and oxidative phosphorylation under conditions where the supply of redox substrates is limited [4]. Gibbs free energy is a nonconserved property that cannot be produced, only imported. It is a necessary commodity, for to allow processes to occur at a nonzero rate, Gibbs free energy must be dissipated. From a functional point of view one might therefore expect biological systems to save as much free energy as possible, i.e., minimize their rates of dissipation of free energy.

Also, Prigogine [5] has shown that at least for systems that are close to equilibrium, entropy production (which is equal to the free energy dissipation divided by the absolute temperature) is minimal in the steady state. Since most biological systems operate about steady states, this may once again suggest that their free-energy dissipation would be very small.

Earlier considerations of optimization of biological free-energy transducers [1,2,6–9] have shown that expectations based on the consideration of a single characteristic of such systems, such

Correspondence address: H.V. Westerhoff, Laboratory of Molecular Biology, National Institute of Diabetes, and Digestive and Kidney Diseases, National Institutes of Health, Building 2, Room 319, Bethesda, MD 20892, U.S.A.

* Present address: NIH, Building 3, Room B1-06, Bethesda, MD 20892, U.S.A.

as their thermodynamic efficiency, are not likely to be realistic. Biological free-energy transducing systems may have additional functions for which they have been optimized and these very optimizations may have required compromises with respect to other criteria of their performance, such as their thermodynamic efficiency.

To see if we can understand the significant free-energy dissipation (entropy production) of actual biological systems along similar lines, we here investigate how a number of other functions of model biological free-energy transducers would vary along with the variation in entropy production, under a number of circumstances. We shall show that near equilibrium, optimal values for most other functions (where we shall focus on efficiency) require significant (i.e., nonminimal) rates of entropy production. By analyzing the specific model of bacteriorhodopsin as a slipping proton pump, we shall demonstrate that similar considerations apply farther from equilibrium. We shall conclude that the possible reason for significant rates of free-energy dissipation in biological free-energy transducers is the fact that they have not (only) been optimized for minimal entropy production, but (also) for other, more mundane, functions, such as efficiency.

2. Results

In this study we shall consider two different models for incompletely coupled free-energy transducers. The first model would be appropriate for the free-energy transducers that catalyze oxidative phosphorylation and are localized in the inner mitochondrial membrane of eucaryotic cells as well as in the plasma membranes of most bacteria [2,10,11]. The input here consists of an oxidation reaction (e.g., that of $NADH + H^+$), the output being the phosphorylation of ADP. We shall consider the free-energy dissipation (i.e., the product of the absolute temperature and the entropy production) ϕ and efficiency η of the free-energy transduction. It should be noted that the free-energy dissipation by processes that may regenerate ADP from ATP will not be included in the evaluation of ϕ and η. We shall resort to this model system to attain general conclusions pertaining to systems that operate near equilibrium.

The second system considered is the light-driven proton pump bacteriorhodopsin [2,12–18]. Here the input is the absorption of photon free-energy [2,15,17,18] by bacteriorhodopsin, whereas the output is the pumping of protons across the membrane against an electrochemical potential difference for protons, $-\Delta\tilde{\mu}_H$ [19]. This model will serve as the special, farther from equilibrium case for which we study the relationship between efficiency and free-energy dissipation. The source of uncoupling will be the slip in its proton pumping [2,14,16,20].

2.1. Near-equilibrium systems

For simplicity we shall confine this study to processes in which an 'input' reaction runs down its own free-energy difference (ΔG_i, which is taken to be positive at a rate J_i) and an 'output' reaction runs against its free-energy difference (ΔG_o, which also is taken as positive) at a positive rate $-J_o$. Reactions i and o have no necessary chemical connection (such as glucose phosphorylation and ATP dephosphorylation in the hexokinase reaction would have).

The overall efficiency η is defined as [1,2,6]:

$$\eta = -J_o\Delta G_o/(J_i\Delta G_i) \quad (1)$$

If the system is in a steady state such that all other reaction rates and transmembrane fluxes are zero, the total rate of free-energy dissipation is given by the dissipation function ϕ [1,2,21]:

$$\sigma_s T = \phi = J_i\Delta G_i + J_o\Delta G_o \quad (2)$$

σ_s is the entropy production function. It is seen that the input reaction contributes a positive term to the dissipation function, whereas the output reaction contributes a negative term (because J_o is negative). The second law of thermodynamics requires that $\eta < 1$ and $\phi > 0$ [1,2,5,21]. One may eliminate the output reaction from eqs. 1 and 2 to obtain a relationship between overall efficiency and free-energy dissipation:

$$\eta = 1 - \phi/(J_i\Delta G_i) \quad (3)$$

In many, though not all, of our considerations the

free energy of the input reaction will be a fixed parameter (cf. refs. 6 and 7). Eq. 3 then testifies to an intuitive notion we had, i.e., that by increasing the free-energy dissipation one will tend to decrease the efficiency. However, this testimony is strict only if J_i, i.e., the rate of the input reaction, remains constant (in oxidative phosphorylation this would correspond to the absence of respiratory control). Therefore, the answer to our question as to whether efficiency decreases when the free-energy dissipation is increased must depend on the extent to which J_i increases with free-energy dissipation. For systems where both ΔG_i and ΔG_o are significantly smaller than RT (i.e., 2.5 kJ/mol) the relations between the flows (reaction rates) and forces (free-energy differences) are proportional and symmetrical allowing for the following phenomenological description [1,6,7,22]:

$$J_i/(L_{ii}\Delta G_i) = 1 + qZ\Delta G_o/\Delta G_i \quad (4)$$

$$J_o/(L_{ii}\Delta G_i) = qZ + Z^2\Delta G_o/\Delta G_i \quad (5)$$

Here L_{ii}, q and Z are determined by the equilibrium state in the vicinity of which the system operates and are independent of ΔG_o and ΔG_i. q and Z have been called the coupling coefficient and the phenomenological stoichiometry, respectively. In our sign convention [2], Z is positive, whereas q lies in between -1 (complete coupling) and 0 (no coupling). With eqs. 4 and 5 the overall efficiency and the free-energy dissipation function, respectively, can be written as [1,2,6]:

$$\eta = -\chi(q+\chi)/(1+q\chi) \quad (6)$$

$$\phi/\left(L_{ii}(\Delta G_i)^2\right) = 1 + 2q\chi + \chi^2 \quad (7)$$

with

$$\chi = Z\Delta G_o/\Delta G_i \quad (8)$$

2.1.1. Varying the output free-energy difference

As one way of varying the free-energy dissipation one may consider varying the free-energy difference of the output reaction [6,7]. At constant values of Z and ΔG_i, this corresponds to varying χ. As shown by Kedem and Caplan [6] the efficiency goes through a maximum at

$$\chi_{opt} = \left(-1 + \sqrt{1-q^2}\right)/q \quad (9)$$

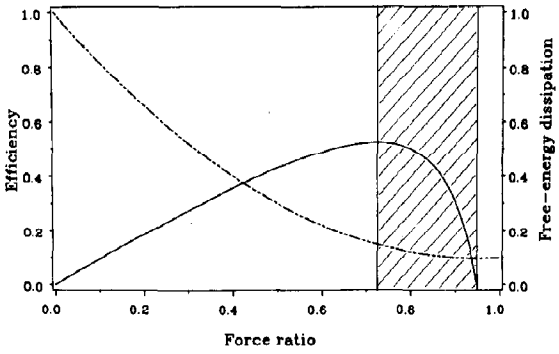

Fig. 1. Free energy conversion for linear relations between flows and forces. Dependence of efficiency η (———) and normalized free-energy dissipation $\phi/(L_{ii}(\Delta G_i)^2)$ (- - - - -) on force ratio χ ($Z = 1$; ΔG_i constant). Plots of eqs. 6 and 7 for the degree of coupling $q = -0.95$. The shaded area between two vertical lines intersecting the x-axis at $\chi = 0.95$ ($\eta = 0$), and at $\chi = \chi_{opt}$ ($\eta = \eta_{max}$), displays both increased efficiency and increased dissipation when the force ratio decreases from its maximal value: $\chi = -q$.

On the other hand, ϕ decreases monotonically with ΔG_o until it reaches a minimum at $\chi = -q$, where the efficiency has already returned to zero. Fig. 1 shows the efficiency η (full line) and (normalized) free-energy dissipation $\phi/(L_{ii}(\Delta G_i)^2)$ as a function of the normalized force ratio χ for a degree of coupling of -0.95. Clearly with this way of varying the free-energy dissipation, the efficiency of free-energy transduction can increase (at $\chi_{opt} < Z\Delta G_o/\Delta G_i < -q$), or decrease (at $0 < Z\Delta G_o/\Delta G_i < \chi_{opt}$) with an increase of overall free-energy dissipation. The region of increased efficiency and free-energy dissipation for decreased force ratio is the shaded area in fig. 1. We conclude that, if the free-energy transduction is to be optimal with respect to efficiency, and if the output force is a parameter than can be varied to improve the efficiency, then the best state is not the state with the lowest possible free-energy dissipation.

As pointed out by Kedem and Caplan [6], biological free-energy transducers may be optimized for functions other than efficiency. We have calculated how, under conditions of varying output force, output functions like output flow ($-J_o$), flow ratio (or yield $-J_o/J_i$), output power ($-J_o\Delta G_o$), efficiency η, economic output flow [2,7] ($-J_o\eta$) and economic output power [2,7]

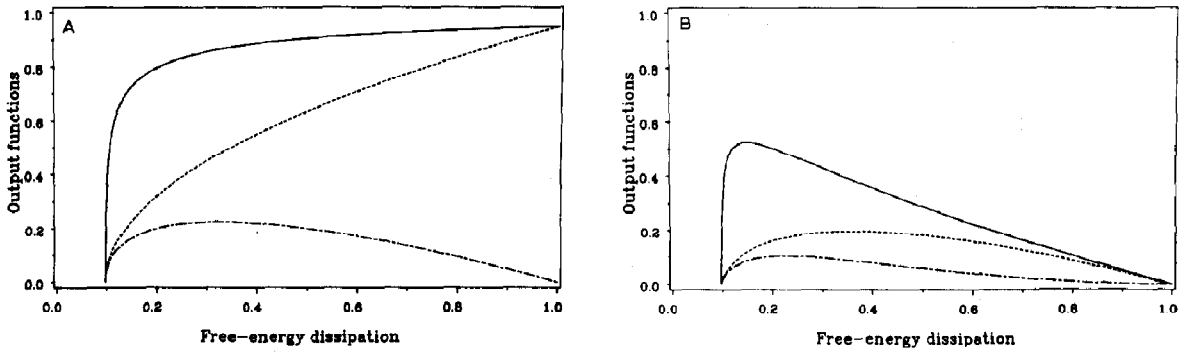

Fig. 2. The variation of several output functions with normalized free-energy dissipation. (A) Normalized output flow $-J_o/(L_{ii}\Delta G_i)$ (———), flow ratio $-J_o/J_i$ (- - - - - -), and normalized output power $-J_o\Delta G_o/(L_{ii}(\Delta G_i)^2)$ (- - - - -) as functions of $\phi/(L_{ii}(\Delta G_i)^2)$ for $Z=1$ and $q=-0.95$. (B) Efficiency η (———), normalized economic output flow $-J_o\eta/(L_{ii}\Delta G_i)$ (- - - - - -) and normalized economic output power $-J_o\Delta G_o\eta/(L_{ii}(\Delta G_i)^2)$ (- - - - -) as functions of $\phi/(L_{ii}(\Delta G_i)^2)$ for $Z=1$ and $q=-0.95$. Eqs. 4–8 were used to plot these functions for the case in which ΔG_o was varied.

$(-J_o\Delta G_o\eta)$ would vary with free-energy dissipation. For the former three, the results are shown in fig. 2A; the latter appear in fig. 2B. Like efficiency (full line in fig. 2B), output power (- - - - - in fig. 2A), economic output flow and economic output power (fig. 2B) would also exhibit a maximum, each at a different magnitude of the rate of free-energy dissipation. The output flow and yield (full and dotted lines, respectively, in fig. 2A) increase monotonically with the rate of entropy production. Significantly, none of these output functions exhibits its maximum at the lowest rate of free-energy dissipation that is attainable at this degree of coupling.

2.1.2. Varying the degree of coupling

Varying the output free-energy difference means that the demand imposed on the free-energy transducer is varied. Thus, one may search for the optimal 'work load'. This strategy, however, does not reveal whether the transducer itself is configured so as to perform optimally under given demands. To uncover this, one needs to vary properties of the transducer at constant magnitude of ΔG_o. The most obvious property of the transducer to be varied is its degree of coupling. A problem arises at this point: in general Z and L_{ii} will vary with q (refs. 2 and 23; see also below). Since there are (special) ways of varying q such that Z and L_{ii} remain constant [2], we may first consider the academic possibility of varying q at constant Z and L_{ii}. Fig. 3 (cf. eqs. 6 and 7) shows that under these conditions efficiency increases monotonically with $|q|$ whereas the normalized free-energy dissipation decreases monotonically with $|q|$. Thus, if q is varied at constant Z and L_{ii}, efficiency increases with decreasing free-energy dissipation.

In general however, Z and L_{ii} will vary as q is varied [2,23]. A mosaic nonequilibrium thermodynamic ('MNET') [2,24] description of the system allows us to be more specific with respect to what we mean if we say we vary the coupling in the system. We shall consider the case [11] where the input reaction (i) is a nonslipping proton pump generating a transmembrane electrochemical potential difference for protons: $\Delta\tilde{\mu}_H$. The output

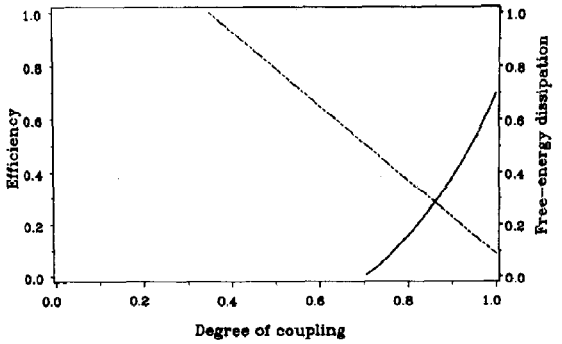

Fig. 3. Dependence of efficiency η (eq. 6) (———) and normalized free-energy dissipation (eq. 7) (- - - - -) on $|q|$ for the force ratio $\chi=0.7$ ($Z=1$).

reaction is a second nonslipping proton pump (o) driven by this $\Delta\tilde{\mu}_H$. As uncoupling element we shall consider a proton leak ℓ in the membrane. Since we confine the discussion to the near-equilibrium domain, the MNET relations [2] reduce to:

$$J_i = L_i(\Delta G_i + n_H^i \Delta\tilde{\mu}_H) \quad (10)$$

$$J_H^i = n_H^i J_i \quad (11)$$

$$J_H^\ell = L_H^\ell \Delta\tilde{\mu}_H \quad (12)$$

$$J_H^o = n_H^o J_o \quad (13)$$

$$J_o = L_o(\Delta G_o + n_H^o \Delta\tilde{\mu}_H) \quad (14)$$

Here J_H^i and J_H^o are the proton fluxes directly coupled to the chemical input and output reaction, respectively, at stoichiometries n_H^i and n_H^o (>0) respectively. J_H^ℓ is the proton flux through the leaks. L_H^ℓ is proportional to the activities and total number of proton leaks. L_i and L_o are proportional to the activities and concentrations of the input and output proton pumps, respectively. In mitochondria J_i, $-J_o$, $-J_H^\ell$, ΔG_i, ΔG_o and $-\Delta\tilde{\mu}_H$ are positive under the usual conditions [2]. L_i, L_o and L_H^ℓ are positive definite.

We shall only be considering steady states in which net proton flow: $J_H = J_H^i + J_H^\ell + J_H^o$ has dwindled to zero. This condition allows us to express $-\Delta\tilde{\mu}_H$ with respect to the other two free-energy differences:

$$\left[(n_H^i)^2 L_i + L_H^\ell + (n_H^o)^2 L_o\right](-\Delta\tilde{\mu}_H) = n_H^o L_o \Delta G_o + n_H^i L_i \Delta G_i \quad (15)$$

Substituting this value for $\Delta\tilde{\mu}_H$ into eqs. 10 and 14 we obtain:

$$J_i/(L_{ii}\Delta G_i) = 1 - x/(1+\Lambda_o) \quad (16)$$

$$J_o/(L_{ii}\Delta G_i) = \left[(n_H^i/n_H^o)/(1+\Lambda_o)\right]\left[x(1+\Lambda_i) - 1\right] \quad (17)$$

where:

$$x = (n_H^i \Delta G_o)/(n_H^o \Delta G_i) \quad (18)$$

$$\Lambda_i = L_H^\ell/\left((n_H^i)^2 L_i\right) \quad (19)$$

$$\Lambda_o = L_H^\ell/\left((n_H^o)^2 L_o\right) \quad (20)$$

and:

$$L_{ii} = L_i(1 + 1/\Lambda_o)/(1 + 1/\Lambda_o + 1/\Lambda_i) \quad (21)$$

These equations are analogues of eqs. 4 and 5. The L_{ii} is now an explicit function of the activities of the input enzyme (L_i), the output enzyme (L_o) and the leak (L_H^ℓ). When the coupling coefficient q and the 'phenomenological stoichiometry' coefficient Z are introduced in order to make eqs. 16 and 17 formally identical to eqs. 4 and 5, respectively, q and Z also become specific functions of L_i, L_o and L_H^ℓ. For q this expression reads [2]:

$$1/q = -\sqrt{(1+\Lambda_i)(1+\Lambda_o)} \quad (22)$$

It follows that, even in the simple model we discuss here, where leakage is the only cause of uncoupling, there is more than one way to vary q. One can increase $-q$ by reducing the proton permeability of the membrane (L_H^ℓ), by increasing the activity or concentration of the input or output proton pumps, or by increasing the proton pumping stoichiometries of these pumps. The expression for Z:

$$Z = (n_H^i/n_H^o)\sqrt{(1+\Lambda_i)/(1+\Lambda_o)} \quad (23)$$

shows that only if $(n_H^i)^2 L_i$ happens to equal $(n_H^o)^2 L_o$ (such that $\Lambda_i = \Lambda_o$) can one vary q at constant Z by solely varying the proton permeability of the membrane.

Using eqs. 16 and 17, the expressions (eqs. 1 and 2) for the overall efficiency and free-energy dissipation become, respectively:

$$\eta = \left[x(1+\Lambda_i) - 1\right]/\left[1 - (1+\Lambda_o)/x\right] \quad (24)$$

$$\phi/\left(L_{ii}(\Delta G_i)^2\right) = 1 - 2x/(1+\Lambda_o) + x^2(1+\Lambda_i)/(1+\Lambda_o) \quad (25)$$

We may now vary ϕ in any of a number of defined ways and see how η varies with it. It can be shown that ϕ is a monotonically increasing function of L_o, L_i and L_H^ℓ. η is a monotonically increasing function of both L_i and L_o, but a monotonically decreasing function of L_H^ℓ. Consequently, if proton leakage is varied, efficiency will decrease with an increase in free-energy dissipation, but if the activity or concentration of either proton pump is varied the free-energy dissipation

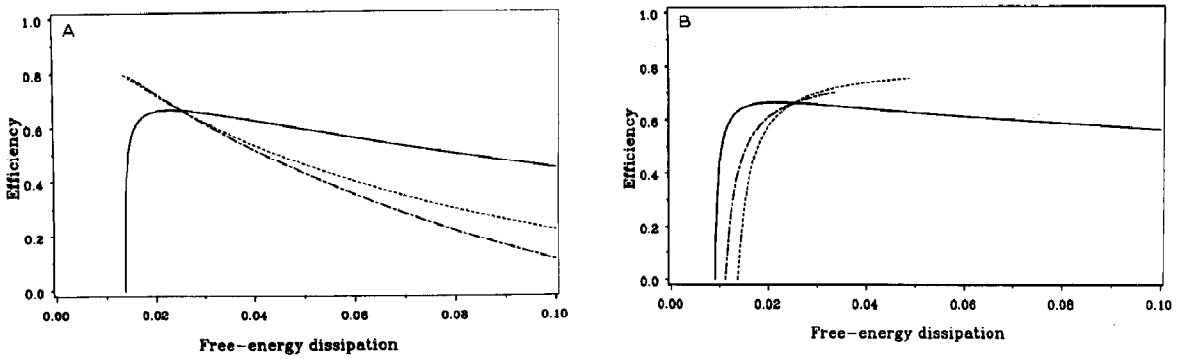

Fig. 4. Variation of efficiency with free-energy dissipation for a near-equilibrium free-energy transducer. (A) Efficiency variation with free-energy dissipation when (a) output force ΔG_o is varied (———), (b) degree of coupling q is varied (here eqs. 6 and 7 were used; - - - - -) and (c) leakage coefficient L'_H is varied (- - - - - -). (B) Efficiency variation with free-energy dissipation when (a) input force is varied (———), (b) L_i is varied (- - - - -), and (c) L_o is varied (- - - - - -). Curves are not drawn past the points at which the parameters would achieve forbidden values: negative for L parameters, $|q| > 1$. Free-energy dissipation was not normalized here; it is in RT units/unit time per unit material. Two nonslipping proton pumps and a proton leak are included in the free-energy transducing proton circuit. The parameters considered are activities and concentrations of the input and output proton pumps and proton leaks, L_i, L_o, and L'_H, respectively, force ratio $x = (n^i_H \Delta G_o)/(n^o_H \Delta G_i)$, and degree of coupling q (eq. 22). Chosen standard-state values for the input and output proton stoichiometries are $n^i_H = 6$ and $n^o_H = 3$, respectively, for force ratio $x = 0.8$, while L coefficients in the standard state are $L_i = 1$, $L_o = 2$, $L'_H = 0.5$. Each parameter was varied in the expression for efficiency (eq. 24) and dissipation (eq. 25), while maintaining the other parameters constant.

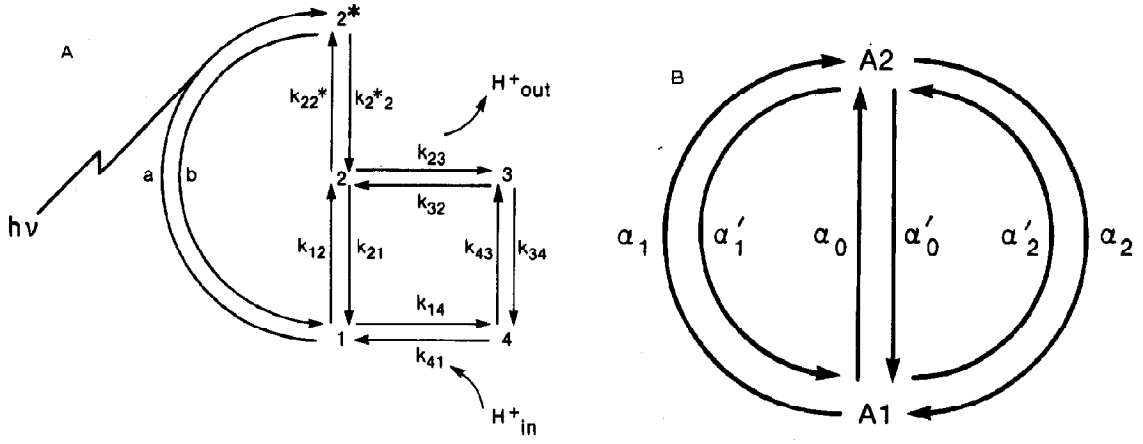

Fig. 5. Model of a light-driven proton pump. (A) Five-state kinetic scheme. Light absorption rate constant a is proportional to the flux density of incoming photons that are reaching the surface of the bacteriorhodopsin-containing membrane. Relaxation of the excited state 2^* occurs either through the internal slip pathway $2^* \rightarrow 2 \rightarrow 1$, or through the productive photocycle $2^* \rightarrow 2 \rightarrow 3 \rightarrow 4 \rightarrow 1$ coupled to proton release (to the external compartment) and proton uptake (from the internal compartment). The equilibrium proton dissociation constants in reactions $2 \rightleftarrows 3$ and $1 \rightleftarrows 4$ are assumed to have such a dependence on proton electrochemical gradient $\Delta\tilde{\mu}_H$, that build-up of the $\Delta\tilde{\mu}_H$ in absolute magnitude (due to photocycling) tends to slow down clockwise cycling. (B) Reduced two-state model. Assuming fast equilibrium for protonation-deprotonation reactions ($2 \rightleftarrows 3$ and $1 \rightleftarrows 4$) and for relaxation from a short-lived excited state ($2^* \rightleftarrows 2$), the five-state kinetic scheme of A can be reduced to this two-state scheme with the state probabilities $p_{A2} = p_2^* + p_2 + p_3$ and $P_{A1} = 1 - p_{A2} = p_1 + p_4$ (appendix A). Here p_1, p_2, p_3, p_4 and p_2^* are probabilities of corresponding states in the five-state kinetic scheme. The connection between reduced rate constants α and original rate constants in the five-state model is given in appendix A.

will increase with increasing efficiency, In fig. 4 we have plotted for a given set of parameter values how efficiency η would vary with free-energy dissipation as ΔG_o (full line), L'_H, q (at constant Z and L_{ii}, see above) (fig. 4A), or ΔG_i (full line), L_o, L_i (fig. 4B) are varied. Significantly, (cf. fig. 4B and full line in fig. 4A), the relationship between η and ϕ can be such that to increase η one would also increase ϕ.

2.2. *Farther from equilibrium*

The farther away from equilibrium, the more the thermodynamic properties of systems are determined by the kinetic parameters [2]. One consequence is that completely general statements become rarer. Since the farther-from-equilibrium case is more of interest for actual biological free-energy transduction, it is important to see if the trends observed above in the near-equilibrium case may persist in farther-from-equilibrium cases that are expected to mimick closely actual biological free-energy transducers.

The kinetics of steady-state, free-energy-transducing systems can be handled by the use of the diagrammatic method [2,25,26]. It is often possible to use a simple, effective diagram, such as that represented in fig. 5B. We show in appendix A that this two-state–three-cycle diagram can be obtained by the process of reduction of the original five-state diagram (fig. 5A) which may model the free-energy transduction by bacteriorhodopsin. The reduction of a diagram [25] takes advantage of the fact that some states of the macromolecule are in reality the transient intermediates and as such have negligible probability, while some neighbouring states are in rapid equilibrium with each other. Our pseudo-two-state model (fig. 5B) can arise from various more complex (and more realistic) kinetic models. For instance, both kinetic models for electrogenic ion pumps (bacteriorhodopsin and H^+-ATPase) described recently by Läuger [27], have equivalent representations in Hill's diagram of fig. 5B [18].

We are concerned with systems that are incompletely coupled. In section 1 this uncoupling consisted of leakage of protons, which partly dissipated the free-energy difference ($-\Delta\tilde{\mu}_H$) linking the input enzyme to the output enzyme. A different cause of uncoupling is slip [2,14,16,20,26]. For the case of bacteriorhodopsin this would mean that [2,14,16,25] either the photochemical reaction would occur without protons being pumped, or (reverse) proton movement would occur without the photochemical reaction being reversed. The distinction between the latter type of slip and leak is that slip is, but leak is not catalyzed by bacteriorhodopsin [2].

Bacteriorhodopsin embedded in a membrane across which there exists a $\Delta\tilde{\mu}_H$ is an incompletely coupled free-energy transducer [14,16,18] and so are mitochondrial electron transfer-linked proton pumps and, H^+-ATPases [20,28]. In the following we shall be interested in relating the free-energy dissipation by bacteriorhodopsin to the thermodynamic efficiency at which it operates.

2.2.1. *Efficiency and free-energy dissipation*

Near equilibrium an important property of the static head state is that it is the state with minimal free-energy dissipation [5]. Such a characterization in terms of free-energy dissipation may not be possible farther away from equilibrium, but we can still regard such a state as a reference state and take it as an origin for the measurement of effective forces that operate in the system (cf. ref. 29).

The definition of the thermodynamic driving force ($\Delta G_i > 0$) associated with photon absorption has been diseussed elsewhere [2,15]. The output force is the proton electrochemical gradient ($\Delta G_o = \Delta\tilde{\mu}_H < 0$). Two effective forces can be introduced (appendix B):

$$X_i = \Delta G_i - \Delta G_i^{shi} \tag{26}$$

$$X_o = \Delta G_o - \Delta G_o^{sho} \tag{27}$$

that vanish when corresponding static head states sho and shi are realized (cf. the appendices). For bacteriorhodopsin the shi state would correspond to the theoretical situation when an equal number of photons is absorbed from the illumination as is reemitted under the influence of the electrochemical proton gradient. (In actual practice the $\Delta\tilde{\mu}_H$ needed to reach the condition of zero input flow, $J_i = 0$, condition would be so large, in its

absolute value, that dielectric breakdown of the membrane would occur.) sho is the more usual 'forward' static head state where for constant input free energy the output flow J_o becomes equal to zero (i.e., zero proton pumping by bacteriorhodopsin; it should be noted that ΔG_o^{sho} is not equal to the output force at static head if the membrane also contains a proton leak; e.g. ref. 19).

The far-from-equilibrium steady-state fluxes conjugate to X_i and X_o are photon absorption current J_i and proton flow across the membrane J_o, respectively:

$$J_i = L_i(\exp(X_i/RT) - 1) \quad (28)$$

$$J_o = L_o(\exp(X_o/RT) - 1) \quad (29)$$

where R and T refer to the gas constant and absolute temperature, respectively. Explicit expressions for coefficients L_i and L_o are given in appendix B (eqs. B15 and B16) [18]. They are functions of all the rate constants (fig. 5A).

From eqs. 26–29, the overall efficiency (eq. 1) and net steady-state rate of free-energy dissipation (eq. 2) in the far-from-equilibrium case are:

$$\eta = -(L_o\Delta G_o/L_i\Delta G_i)(\exp(X_o/RT) - 1)/(\exp(X_i/RT) - 1) \quad (30)$$

$$\phi = (1-\eta)L_i\Delta G_i(\exp(X_i/RT) - 1) \quad (31)$$

2.2.2. *Varying the input and output forces*

Fig. 6 shows the efficiency η, the free-energy dissipation $J_i\Delta G_i$ due to input processes, and $J_i\Delta G_i + J_o\Delta G_o$, the total free-energy dissipation, as

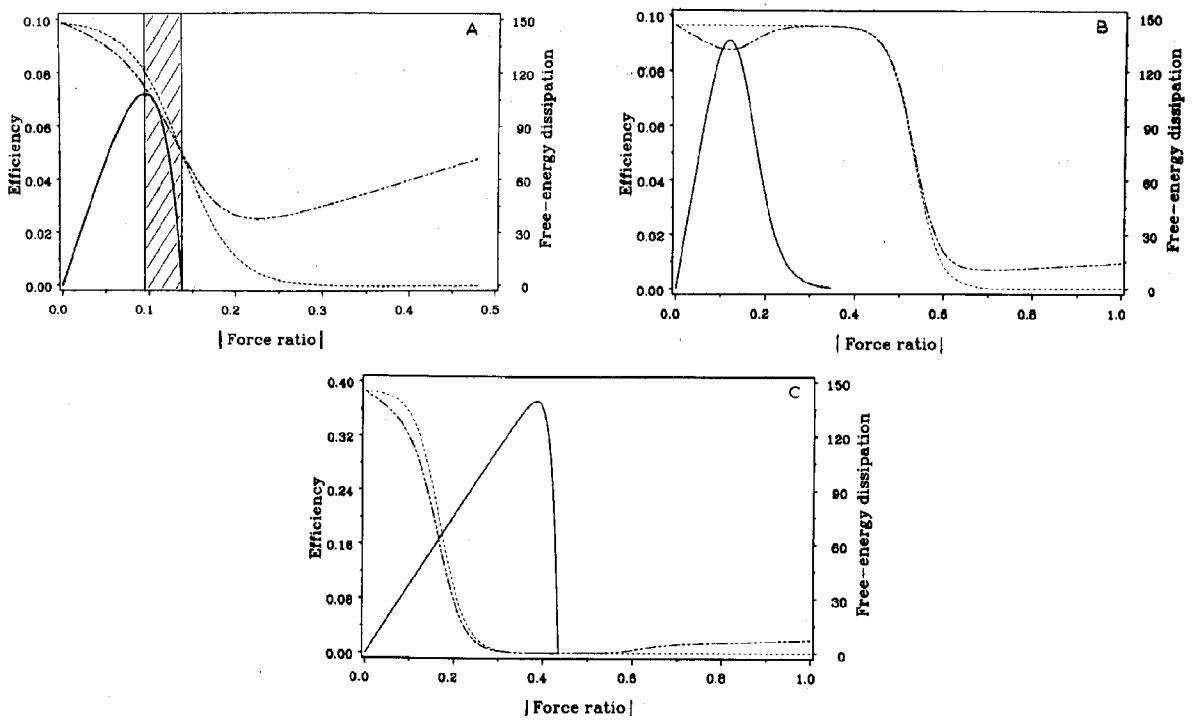

Fig. 6. Dependence of efficiency and normalized free-energy dissipation on absolute force ratio (with constant input force) for the light-activated proton pump kinetic scheme assumed to model the bacteriorhodopsin proton pumping (fig. 5). The equations used to plot the steady-state values of overall efficiency (———) (eq. 30), net free-energy dissipation (- - - - -) (eq. 31 normalized by $N_o k_{12}(\Delta G_i)^2/RT$) and contribution $J_i\Delta G_i$ of the input process to the net free-energy dissipation (- - - - - -) (eq. 31 with $\eta = 0$ and normalized by $N_o k_{12}(\Delta G_i)^2/RT$) are not restricted to the near-equilibrium region. The parameters of the simulation were as follows: (A) $a = 1$, $b = 10^9$, $k_{43} = 1$, $k_{34} = 10^4$, $k_{12} = 10^{-4}$, $k_{21} = 10^8$, $c' = c'' = c$, $\bar{K}_E/c = 10^6$, $\bar{K}_I/c = 10^{-2}$, $B = 10^{-26}$, $Q = 10^{-38}$; (B) as in panel A except for $a = 10$, $k_{43} = 10^3$, $k_{34} = 10^7$, $k_{12} = 5\times10^{-8}$, $k_{21} = 5\times10^4$, $\bar{K}_E/c = 1$, $\bar{K}_I/c = 10^{-8}$, $B = 10^{-23}$, $Q = 10^{-35}$; (C) as in panel B except for $k_{12} = 10^{-9}$, $k_{21} = 10^3$, $\bar{K}_I/c = 0.003$, $\bar{K}_E/c = 3\times10^5$.

functions of the force ratio $|\Delta G_o/\Delta G_i|$, when only ΔG_o is varied. The free-energy dissipations have been normalized with the constant factor $N_o k_{12}(\Delta G_i)^2/RT$, where N_o is the number of bacteriorhodopsins in the membrane and k_{12} one of the internal slip rate constants (fig. 5A). Minima in the total (normalized) free-energy dissipation do not coincide (in general) with the static head state condition (indicated in fig. 6A by the second vertical line passing through the point of zero efficiency and by the end of the full line). Here we find a deviation from the property near-equilibrium systems have, i.e., that their state of minimal free-energy dissipation coincides with the static head steady state [5]. Interestingly (see, for instance, fig. 6B), the free-energy dissipation as a function of the output force exhibits multiple minima in some cases.

In practice, the output force (in this case the electrochemical proton gradient) can be decreased (in absolute value) by adding a 'load', i.e., an enzyme that would consume part of $\Delta\tilde{\mu}_H$. As $|\Delta\tilde{\mu}_H|$ would thus decrease, its back pressure [16,19] on the proton pump would be alleviated and $-J_o$ would increase rather strongly. This would tend to diminish the dissipation of free energy. However, if (as is the case in fig. 6A) the input flow is also sensitive to back pressure, an increase in the term $J_i\Delta G_i$ may outweigh the decrease in $J_o\Delta G_o$, such that the free-energy dissipation increases with decreasing $|\Delta\tilde{\mu}_H|$. This is illustrated by the dashed line; the normalized $J_i\Delta G_i$ (- - - - - -) in fig. 6A increases more than the normalized ϕ as $|\Delta\tilde{\mu}_H|$ is lowered.

Back pressure of the output force on the input flow is found at least in some proton pups, such as the mitochondrial respiratory chain [2,30]. However, it does not seem to be a strong attribute of all proton pumps: the *E. coli* electron transfer may be much less sensitive to $\Delta\tilde{\mu}_H$. Also, for bacteriorhodopsin it has been suggested [2,16] that its input flux (i.e., the rate at which it absorbs photons) may be hardly affected by $\Delta\tilde{\mu}_H$. Of such proton pumps fig. 6B would be representative. Here it is seen that one minimum in the free-energy dissipation occurs at $\Delta\tilde{\mu}_H$ values below the static head value. The difference between the cases of fig. 6A and B lies in the values for the kinetic

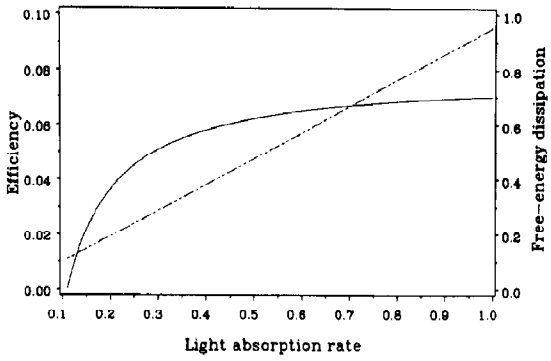

Fig. 7. Simulation results for the proton pump model (fig. 5) when light absorption rate a is varied. Efficiency η (———) (eq. 30) and net free-energy dissipation (- - - - -) (eq. 31 normalized by $N_o(\Delta G_o)^2/RT$) are plotted for the same choice of parameters as in fig. 6A. Output force was maintained at $-7RT$.

constants of the catalytic cycle of the proton pump.

For the second type of proton pump, the free-energy dissipation decreases as $|\Delta\tilde{\mu}_H|$ is lowered starting from its static head value. Thus, the variation of free-energy dissipation with efficiency appears to depend on the strength of the back-pressure effect. It should be noted that in the case of fig. 6B there is a second minimum in the free-energy dissipation near a normalized force ratio of 0.7 and a maximum close to but not at the static head. When the rate constants for the slip pathway are reduced, the minima in free-energy dissipation shift to the static head (fig. 6C).

Instead of varying ΔG_o with ΔG_i constant, it is also possible to vary ΔG_i (by varying the light intensity) and to keep ΔG_o clamped at a desired value giving nonzero efficiency. The results for η and $\phi/(N_o(\Delta G_o)^2/RT)$ are shown in fig. 7. The minimal light intensity needed to have $\eta > 0$ depends on the choice of ΔG_o. Both η and normalized free-energy dissipation increase for increased light intensity.

In fig. 8 we have plotted the variation of the free-energy dissipation with efficiency for the above two ways of varying the properties of the system; (———) for varying ΔG_o and (— — —) for varying ΔG_i. The same figure also includes the relationships obtained when the catalytic properties of the pump are changed in two different

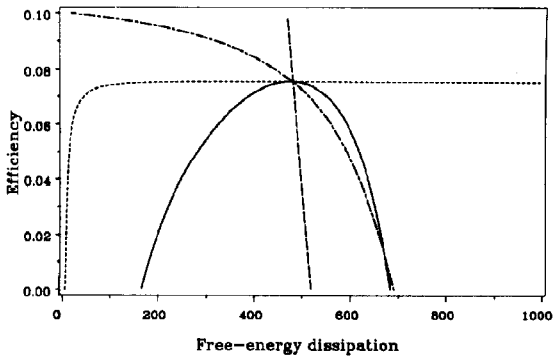

Fig. 8. Variation of efficiency with free-energy dissipation for the bacteriorhodopsin model when (a) output force ΔG_o is varied (———) from −11.55 to 0 (in RT units), (b) light absorption rate a is varied (- - - - -) from 0.1 to 20.5, (c) the equilibrium constant for the protonation reaction, k_{14}/k_{41}, is varied (-----) from 3 to 10^{-8} (with, because of microscopic reversibility (A_B), k_{23}/k_{32} being varied by the same factor), (d) rate constant k_{12} or k_{34} is varied (— — —) from 10^{-5} to 0.009 and from 10^6 to 1, respectively, in such a way that ratios $k_{12}/k_{21}=10^{-12}$ and $k_{34}/k_{43}=10^4$ did not change. Free-energy dissipation is normalized with N_o. Rate constants and forces kept constant in this simulation are: $a=10$, $B=10^{-26}$, $b=10^9$, $k_{12}=10^{-4}$, $k_{21}=10^8$, $k_{34}=10^4$, $k_{43}=1$, $\bar{K}_I/c=10^{-2}$, $\bar{K}_E/c=10^6$, $\Delta G_o=-7.0$ (in RT units). Free-energy dissipation is in RT units/unit time per unit material.

ways, i.e., by varying the acid dissociation constants (- - - - -), or by varying the pump's propensity to slip (— — —) (cf. fig. 5A). We conclude that also for the case of the farther-from-equilibrium proton pump free-energy dissipation can increase with increasing efficiency, i.e., in the case where the output force is varied and in the case where the input force is varied.

3. Discussion

We have shown that the way in which efficiency varies with free-energy dissipation depends on how the properties of the free-energy transducing system are varied. When, within a free-energy transducing system consisting of two separate enzymes (such as is the case in chemiosmotic coupling [2]) leakage is increased, efficiency tends to dwindle with increasing free-energy dissipation. However, when the free-energy transducing enzymes (the proton pumps in chemiosmotic coupling) are fortified, the increase in efficiency tends to be accompanied by an increase in free-energy dissipation.

Also, with the model for the slipping proton pump we observed that free-energy dissipation and efficiency increased together either when changing the input force, or when changing the output force. We conclude that minimum free-energy dissipation and maximum efficiency are generally not attained simultaneously (cf. figs. 4 and 8). Thus, to have maximum efficiency, a free-energy transducing system will have to forsake the possibility of having minimal free-energy dissipation. Vice versa, to have minimal free-energy dissipation, a free-energy transducer will have to function at an efficiency smaller than it might otherwise achieve. Conceivably, an organism would find a compromise with neither the efficiency nor the free-energy dissipation being optimal.

These conclusions are entirely consistent with the analyses by Stucki [7]. He proposed that, in order to optimize with respect to two output functions, two parameters (in ref. 7; the output force and the degree of coupling) should be considered adjustable. Thus, Stucki [7] found optimal states, which would have the maximal value for any out of four output functions (e.g., the output flow) at optimal efficiency, the latter optimum being kept by continuously adjusting the output force to the varying degree of coupling. Also, there the result was a compromise; although the output function and the efficiency would be maximal within the optimization strategy considered, higher magnitudes for either separately could be attained [2,7]. The correspondence between experimental results [2,7,8,31] and the calculations [7] suggest that in nature this type of compromise may be what is achieved.

The conclusion that in the near-equilibrium system the free-energy dissipation (and hence the entropy production) would not be minimal at the steady state, may seem to be at variance with the theorem of minimal entropy production in near-equilibrium steady states [5]. This is merely a paradox, however; entropy production in near-equilibrium steady states is at a minimum only with respect to variation of variable thermody-

namic forces, not with respect to variations in parameters (such as the phenomenological coefficients L_{ij}) [5,21]. When we varied the output force we did find a minimum free-energy dissipation at the (static head) steady state (where $J_o = 0$; fig. 1). It was only as we varied catalytic properties of the free-energy transducing system (such as q; fig. 3) that the minimum free-energy dissipation no longer coincided with zero output flux (see, for instance, fig. 3).

Prigogine's theorem of minimum free-energy dissipation in the steady state [5] was limited explicitly to near-equilibrium situations. The results of our calculations for the far-from-equilibrium free-energy transducer (which might come close to modelling bacteriorhodopsin) demonstrate that far from equilibrium the free-energy dissipation may be minimal (with respect to variations in the output force) away from the steady state (cf. fig. 6A and B). Fig. 6C shows that this result is not always obtained; also far from equilibrium minimum free-energy dissipation may be attained at the static head steady state. Fig. 6C, however, is a case where there was relatively little slip in bacteriorhodopsin. Thus, the static head there corresponds to something rather similar to equilibrium (cf. ref. 29).

The present considerations may be relevant for various metabolic contexts in suggesting that one should not expect metabolism to be maximally efficient and minimally wasteful of free energy. As we have shown, these two properties tend to exclude each other. Moreover, processes that expend extra free energy can be useful in improving the extent to which metabolism can be regulated [2,32,33].

For the cases where the growth of organisms was strongly limited by the supply of free energy, optimization in the sense of reducing free-energy dissipation and increasing the thermodynamic efficiency may have been a criterion for evolution (cf. ref. 8). From the present analysis one may deduce that in such a case selection pressure would have worked so as to decrease leakage. When this possibility reached its limit, however, variation of the activity of input or output free-energy transduction catalysis would have had the result of either decreasing free-energy dissipation or decreasing efficiency. The only attainable result would thus have been the status quo with both a significant free-energy dissipation and a submaximal efficiency.

Appendix A: The model for the light-activated proton pump and its reduction to a two-state Hill diagram

We shall use here Läuger's [27] model (fig. 5A) for the bacteriorhodopsin cycle (represented in the form of a Hill diagram [25]). States 1, 2, 3 and 4 can be tentatively assigned to BR_{570}, L_{550}, M_{412} and the O_{640} intermediates. It is thought that the proton-release step from the chromophore takes place between L_{550} and M_{412} and the proton-association step between O_{640} and BR_{570} [12]. Protons are pumped outward if pathway $2 \rightarrow 3 \rightarrow 4 \rightarrow 1$ is used. The free energy of the excited state 2^*, can also be dissipated through the internal slip pathway $2^* \rightarrow 2 \rightarrow 1$.

The overall excitation rate constant a for the transition $1 \rightarrow 2^*$ is

$$a = a_o + \sigma(J_s + J) \tag{A1}$$

where a_o is the rate for the radiationless transition, σ the absorption cross-section of bacteriorhodopsin in state 1 for radiation of frequency ν, J_s the flux density of quanta emitted by the radiation source and impinging on the surface of the bacteriorhodopsin-containing membrane, and J the total ambient flux density of ambient temperature T. An equivalent black-body source with a well-defined radiation temperature T_s can be assigned to the radiation source by using Planck's treatment [34] of nonequilibrium radiation [2,15,27]. When the radiation source with the effective temperature $T_s \gg T$ is switched on, σJ_s becomes the dominant term in eq. A1.

The overall rate constant b for the $2^* \rightarrow 1$ transition is [2,15,27]:

$$b = b_o + b_f + \sigma(J_s + J) \tag{A2}$$

where b_o is the rate for the radiationless process, b_f that for spontaneous emission of photons and $\sigma(J_s + J)$ the rate for induced emission (for which

the rate constant must be equal to that for induced absorption), which can be neglected in this equation at normal light intensities: $b \sim b_o + b_f$.

In the dark, equilibrium at ambient temperature T requires that

$$a_o/b_o = \exp(-h\nu/kT) = Q \tag{A3}$$

where k is Boltzmann's constant.

When all nonradiative and nonproton-pumping transitions between states $2^* \rightleftarrows 1$ and $2 \rightleftarrows 1$ can be neglected ($a_o = b_o = k_{12} = k_{21} = 0$) the proton pump becomes completely coupled. In this case (an isotropic radiation source is also assumed) light free energy can be transformed with maximal yield.

In this model proton translocation through the membrane causes a conformational change, which lowers the potential energy barrier for the release of a proton to the external compartment. The deprotonation reaction ($2 \rightleftarrows 3$) is assumed to be fast with the equilibrium constant:

$$K_E = k_{23}/(k_{32}/c'') \tag{A4}$$

where c'' is the proton concentration in the external compartment. Protonation reaction $4 \rightleftarrows 1$ is also assumed to be fast with the equilibrium constant:

$$K_I = k_{14}/(k_{41}/c') \tag{A5}$$

c' being the proton concentration in the internal compartment. Rate constants k_{32} and k_{41} are the pseudo-unimolecular rate constants, i.e., they are proportional to c'' and c', respectively. K_E and K_I are, as usual, independent of pH. Fast equilibrium is also assumed between the short-lived states 2^* and 2:

$$B = k_{22^*}/k_{2^*2} \tag{A6}$$

Rapid equilibrium (eqs. A4–A6) has the effect of reducing five states in the model (fig. 5A) to only two (fig. 5B) with effective rate constants:

$$\begin{aligned} \alpha_0 &= k_{12}\theta'; & \alpha_0' &= k_{21}\theta'' \\ \alpha_1 &= a\theta'; & \alpha_1' &= bB\theta'' \\ \alpha_2 &= k_{34}K_E\theta''/c''; & \alpha_2' &= k_{43}(1-\theta') \end{aligned} \tag{A7}$$

where

$$\theta' = (1 + K_I/c')^{-1};\ \theta'' = (1 + B + K_E/c'')^{-1} \tag{A8}$$

For each couple of 'fast equilibrium' states we now have a single intermediate state. This reduction procedure has been described by Hill [25].

For simplicity we have assumed that there is only one proton-binding site. The only $\Delta\tilde{\mu}_H$-dependent quantities are assumed to be the equilibrium dissociation constants K_I and K_E:

$$\begin{aligned} K_I &= \bar{K}_I \exp(-F\Delta\psi/2RT); \\ K_E &= \bar{K}_E \exp(F\Delta\psi/2RT) \end{aligned} \tag{A9}$$

where $\bar{K}_I$ and $\bar{K}_E$ are the values of K_I and K_E for $F\Delta\psi = 0$. This implies either a symmetric proton-well situation [35] where $\Delta\psi$ is locally translated to ΔpH, or the complete absence of the $\Delta\psi$ component as in the presence of valinomycin and excess K^+, or in bacteriorhodopsin liposomes in KCl [19].

Appendix B: The flux-force relationships

In Hill's formalism [25] the thermodynamic driving forces are associated with the products of rate constants in closed circles of the basic diagram (fig. 5):

$$\alpha_1\alpha_0'/\alpha_0\alpha_1' = a/bQ = \exp(\Delta G_i/RT) \tag{B1}$$

$$\begin{aligned} \alpha_0\alpha_2/\alpha_0'\alpha_2' &= (c'/c'')\exp(F\Delta\psi/RT) \\ &= \exp(\Delta G_o/RT) \end{aligned} \tag{B2}$$

We have used here the principle of microscopic reversibility, which requires that in the absence of driving forces:

$$Q/B = k_{12}/k_{21} \tag{B3}$$

and

$$\bar{K}_E k_{12} k_{34} = \bar{K}_I k_{21} k_{43} \tag{B4}$$

Note from eqs. A3 and B1 that the input driving force ΔG_i is:

$$\Delta G_i = N_a h\nu + RT \ln(a/b) \tag{B5}$$

where N_a is Avogadro's number. As in refs. 2 and 15, we find that the 'light force' per absorbed

photon is less than the photon energy (for, $a < b$). Eq. 6 from ref. 15, for ΔG_i associated with photon absorption, becomes approximately equal to eq. B5, when transitions $\sigma J_s k_{41} k_{34} k_{23}$ and $(b_f + b_o) k_{41} k_{34} k_{23}$ are dominant contributions to the occupational probabilities p_{2*} and p_1, respectively.

The net proton flux is:

$$J_o = N_o[(\alpha_0 + \alpha_1)\alpha_2 - \alpha_2'(\alpha_1' + \alpha_0')]/\sum \quad \text{(B6)}$$

where

$$\sum = \alpha_0 + \alpha_1 + \alpha_2 + \alpha_0' + \alpha_1' + \alpha_2' \quad \text{(B7)}$$

Using eqs. B1 and B2 we find:

$$J_o = N_o \alpha_2'(\alpha_1' + \alpha_0')(\exp(X_o/RT) - 1)/\sum \quad \text{(B8)}$$

with X_o defined in eq. 27.

The net absorption rate for photons is:

$$J_i = N_o[\alpha_1(\alpha_0' + \alpha_2) - \alpha_1'(\alpha_0 + \alpha_2')]/\sum \quad \text{(B9)}$$

As above we find:

$$J_i = N_o \alpha_1'(\alpha_0 + \alpha_2')(\exp(X_i/RT) - 1)/\sum \quad \text{(B10)}$$

with X_i defined in eq. 26.

From eqs. B6 and B9 reversal potential values in static head steady states sho ($J_o = 0$) and shi ($J_i = 0$) are, respectively:

$$\Delta G_o^{sho} = RT \ln((S_o + 1)/(S_o + \exp(\Delta G_i/RT))) \quad \text{(B11)}$$

$$\Delta G_i^{shi} = RT \ln((S_i + 1)/(S_i + \exp(\Delta G_o/RT))) \quad \text{(B12)}$$

with the 'slip coefficients' S_o and S_i defined by:

$$S_o = \alpha_0'/\alpha_1' = k_{21}/bB \quad \text{(B13)}$$

and

$$S_i = \alpha_0/\alpha_2' = k_{12}c'/k_{43}K_1 \quad \text{(B14)}$$

The coefficients L_o and L_i in eqs. 28 and 29, respectively, can be expressed in terms of rate constants by using eqs. A7, A8, B7, B8, B10, B13 and B14:

$$L_o = N_o bBk_{12}(1 + S_o)/S_i D \quad \text{(B15)}$$

$$L_i = N_o bBk_{12}(1 + 1/S_i)/D \quad \text{(B16)}$$

where

$$D = (1 + B + K_E/c'')(a + k_{12} + k_{43}K_1/c') + (1 + K_1/c')(k_{21} + bB + k_{34}K_E/c'') \quad \text{(B17)}$$

Acknowledgements

We thank Drs. R.D. Astumian, Y. Chen, R.W. Hendler and F. Kamp for discussions. This work was supported in part by National Science Foundation Grant PCM-8443154 and Uniformed Services University Grant GM7160, as well as by the Netherlands Organization for the Advancement of Pure Research (Z.W.O.).

References

1 S.R. Caplan and A. Essig, Bioenergetics and linear non-equilibrium thermodynamics (Harvard University Press, Cambridge, MA, U.S.A., 1983).
2 H.V. Westerhoff and K. van Dam, Thermodynamics and control of biological free energy transduction (Elsevier, Amsterdam, 1987).
3 A.H. Stouthamer, Int. Rev. Biochem. 21 (1979) 1.
4 K. van Dam, H.V. Westerhoff, M. Rutgers, J.A. Bode, P.C. de Jonge, M.M. Bos and G. van den Berg, in: Vectorial reactions in electron and ion transport in mitochondria and bacteria, eds. F. Palmieri, E. Quagliariello, N. Siliprandi and E.C. Slater (Elsevier, Amsterdam, 1981) p. 389.
5 I. Prigogine, Introduction to thermodynamics of irreversible processes (Interscience, New York, 1961).
6 O. Kedem and S.R. Caplan, Trans. Faraday Soc. 21 (1965) 1897.
7 J.W. Stucki, Eur. J. Biochem. 109 (1980) 269.
8 H.V. Westerhoff, K.J. Hellingwerf and K. van Dam, Proc. Natl. Acad. Sci. U.S.A. 80 (1983) 305.
9 J.W. Stucki, M. Compiani and S.R. Caplan, Biophys. Chem. 18 (1983) 101.
10 D.G. Nicholls, Bioenergetics (Academic Press, London, 1982).
11 P. Mitchell, Nature 191 (1961) 144.
12 M. Eisenbach and S.R. Caplan, Curr. Top. Membranes Transp. 12 (1979) 165.
13 J.K. Lanyi, in: Bioenergetics, ed. L. Ernster (Elsevier, Amsterdam 1984) p. 315.
14 S.R. Caplan, in: Dynamic aspects of biopolyelectrolytes and biomembranes, ed. F. Oosawa (Kodansha, Tokyo, 1982) p. 431.
15 D. Juretić, J. Theor. Biol. 106 (1984) 315.
16 H.V. Westerhoff and Z. Dancsházy, Trends Biochem. Sci. 9 (1984) 112.

17 D. Juretić, Croat. Chem. Acta 56 (1983) 383.
18 D. Juretić and F. Sokolić, Croat. Chem. Acta 59 (1986) 599.
19 K.J. Hellingwerf, J.C. Arents, B.J. Scholte and H.V. Westerhoff, Biochim. Biophys. Acta 547 (1979) 561.
20 D. Pietrobon, G.F. Azzone and D. Walz, Eur. J. Biochem. 117 (1981) 389.
21 A. Katchalski and P.F. Curran, Non-equilibrium thermodynamics in biophysics (Harvard University Press, Cambridge, MA, 1967).
22 L. Onsager, Phys. Rev. 37 (1931) 405.
23 D. Walz, Biochim. Biophys. Acta 505 (1979) 279.
24 H.V. Westerhoff and K. van Dam, Curr. Top. Bioenerg. 9 (1979) 1.
25 T.L. Hill, Free energy transduction in biology (Academic Press, New York, 1977).
26 D. Pietrobon and S.R. Caplan, Biochemistry 24 (1985) 5764.
27 P. Läuger, Biochim. Biophys. Acta 779 (1984) 307.
28 M. Zoratti, M. Favaron, D. Pietrobon and G.F. Azzone, Biochemistry 25 (1986) 760.
29 S.R. Caplan, Proc. Natl. Acad. Sci. U.S.A. 78 (1981) 4314.
30 E. Padan and H. Rottenberg, Eur. J. Biochem. 40 (1973) 431.
31 J.W. Stucki and S. Soboll, EBEC Rep. 4 (1986) 18.
32 B. Crabtree and E.A. Newsholme, Curr. Top. Cell. Regul. 25 (1985) 21.
33 A. Sorribas and R. Bartrons, Eur. J. Biochem. 158 (1986) 107.
34 M. Planck, Theorie der wärmestrahlung (Johann Ambrosius Barth, Leipzig, 1923).
35 P. Mitchell, Chemiosmotic coupling and energy transduction (Glynn Research, Bodmin, England, 1968).